JACS
JOURNAL OF THE AMERICAN CHEMICAL SOCIETY
Article
pubs.acs.org/JACS

Enhancing the Emissive Properties of Poly(*p*-phenylenevinylene)-Conjugated Polyelectrolyte-Coated SiO_2 Nanoparticles

Hsiao-Wei Liu, An Thien Ngo, and Gonzalo Cosa*

Department of Chemistry and Centre for Self-Assembled Chemical Structures (CSACS/CRMAA), McGill University, 801 Sherbrooke Street West, Montreal, Quebec H3A 2K6, Canada

Supporting Information

ABSTRACT: Here we describe single-particle imaging studies conducted on the conjugated polyelecrolyte poly[5-methoxy-2-(3-sulfopropoxy)-1,4-phenylenevinylene] (MPS-PPV) supported on SiO_2 nanoparticles. The particles are subjected to a time-programmed sequence involving addition and removal of different additives, including excited-triplet-state quenchers and scavengers of singlet oxygen as well as ground-state oxygen. Our studies show that these additives enhance the emission intensity and photostability of the nanoparticles and may further repair photodamaged conjugated polymer. The ability to monitor the emission from individual particles along multiple cycles under a range of conditions provides a mechanistic insight into the action of these additives.

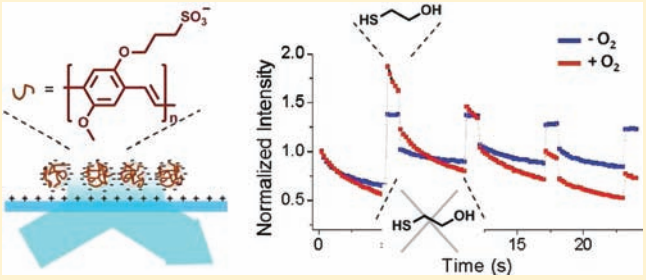

INTRODUCTION

Photodamage of conjugated polymers is a major limitation toward single-molecule/particle studies on polymer photophysics[1] and has prevented the formulation of single-molecule-based assays relying on the emissive properties of these materials. Extensive irradiation of conjugated polymers results in their photodegradation and loss of emission in an oxygen-dependent manner. In the case of light-emitting polymers with a poly(*p*-phenylenevinylene) (PPV) backbone, such degradation occurs mostly through the reaction of singlet oxygen, which is typically sensitized from the triplet excited state of the chromophore.[2] Cycloaddition of singlet oxygen to the vinyl group along the conjugated chain generates a dioxetane which next cleaves, resulting in polymer chain scission and generation of carbonyl defects (see Scheme 1).[2b,3] Carbonyl defects[4] and dioxetanes[5] may act as acceptor groups in photoinduced electon transfer processes between the chains, thus causing the fluorescence loss of the polymers.[4,6] Charged radical species formed along the polymer backbone following reaction with molecular oxygen have also been shown to be involved in the oxidative photodegradation of PPV polymers.[7]

Scheme 1. Mechanism of Singlet Oxygen Mediated Decomposition of PPV Polymers[a]

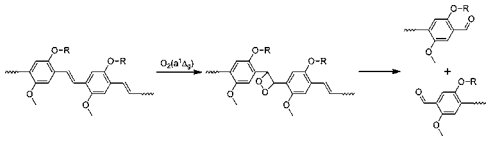

[a]Adapted from ref 2b. Copyright 1995 American Chemical Society.

A number of protocols have been formulated to increase the photostability and enhance the luminescence of fluorophores in single-molecule spectroscopy/biophysical studies.[8] These protocols rely on the addition of water-soluble excited-triplet-state quenchers which may act either via spin−orbit coupling, such as *β*-mercaptoethanol,[9] or via electron transfer to/from the excited triplet state followed by rapid back electron transfer,[10] which is the case for Trolox (6-hydroxy-2,5,7,8-tetramethylchroman-2-carboxylic acid) and its oxidized chromoquinone form.[8b,11] These protocols also exploit singlet oxygen scavengers such as sodium azide or ascorbic acid.[12] Ground-state oxygen scavengers based on the combined action of glucose oxidase and catalase[13] are also commonly employed. Recently, organic-soluble, small-molecule additives designed especially to function as excited-triplet-state quenchers or singlet oxygen quenchers have been shown to greatly increase the photostability of hydrophobic poly(*p*-phenyleneethynylene) (PPE) thin films.[14]

Here we describe a single-molecule/particle approach we have developed to study the fluorescence-enhancing potential, and associated action mechanisms, of a number of additives on the fluorescence performance of nanoparticles consisting of the PPV-based conjugated polyelectrolyte poly[5-methoxy-2-(3-sulfopropoxy)-1,4-phenylenevinylene] (MPS-PPV) supported on SiO_2 nanobeads. Our approach relies on a time-programmed sequence involving addition and removal of the different additives while simultaneously monitoring the emission intensity of the individual nanoparticles over time. The additives studied include ascorbic acid, sodium azide, *β*-

Received: September 7, 2011
Published: December 19, 2011

   dx.doi.org/10.1021/ja208437e | J. Am. Chem.Soc. 2012, 134, 1648−1652

mercaptoethanol, and enzymatic ground-state oxygen scavengers. Our single-molecule/particle results provide a mechanistic insight into the action of these additives and further highlight the potential of using MPS-PPV supported on SiO_2 nanobeads as reactors/sensors for photophysical and photochemical studies.

RESULTS AND DISCUSSION

We first functionalized 100 nm SiO_2 beads with aminosilane groups to render them cationic. The polyanionic MPS-PPV was next deposited via electrostatic interactions[15] onto the beads; we estimate a final value of 69% coverage of the bead surface calculated assuming one MPS-PPV monomer per 0.36 nm^2 of bead surface (see the Supporting Information for details).[16] This platform provides a well-controlled environment with increased polymer backbone interaction allowing for faster exciton transport and thus greater sensitivity in the conjugated polymer.[17] It also enables immobilizing discrete luminescent particles onto the glass substrate for single-molecule/particle imaging. Furthermore, the MPS-PPV polymer coated onto nanobeads is less prone to undergo conformational changes (and concomitant emission changes) induced by nonspecific interactions with proteins in comparison to free polymer in solution.[16] As a result, fluorescence fluctuations in the nanobeads report specific photochemical reactions/photophysical interactions between MPS-PPV and additives, rather than additive-induced conformational changes on MPS-PPV.

To study the effect of the various additives on MPS-PPV-coated SiO_2 nanobeads, we adsorbed the MPS-PPV shell/SiO_2 core nanoparticles onto the surface of aminosilanized glass coverslips in a 10 μL flow chamber to perform fluorescence imaging under various conditions. Using a total internal reflection fluorescence (TIRF) microscopy setup provided with a charge-coupled device (CCD) camera and a 488 nm Ar^+ laser, the emission intensity of individual MPS-PPV-coated nanobeads was monitored at a repetition rate of 5 Hz. Hundreds of particles were simultaneously monitored along consecutive cycles of a programmed sequence involving a 5 s illumination in buffer solution, a thorough rinse with the additive-containing solution in the dark, a 1 s illumination in the additive solution, and a thorough rinse with buffer solution in the dark (see the Supporting Information for further details). The choice of 5 s of continued irradiation in buffer solution was based on the observed time dependence for photobleaching under our experimental conditions. Upon recording the individual particle emission intensity over time trajectories and combining them into an ensemble average trajectory, we determined that photobleaching followed a biexponential decay function with characteristic lifetimes of 4.3 and 40 s and preexponential factors of 60% and 40%, respectively (see the Supporting Information, Figure S1). (This would be consistent with the rapid O_2-mediated destruction of low-energy longer segments where energy is efficiently funneled, followed by the slower destruction of high-energy shorter segments.)[18] We thus chose to irradiate for the duration of ca. 1 lifetime of the rapid photobleaching. Furthermore, a 1 s illumination upon additive addition responded to the need of minimizing photobleaching under these conditions.

We first acquired images on immobilized MPS-PPV-coated nanobeads in consecutive cycles involving addition and removal of 143 mM β-mercaptoethanol in air-equilibrated solutions (movie S1 in the Supporting Information). Panels A and B of Figure 1 display two such images before and after addition of β-

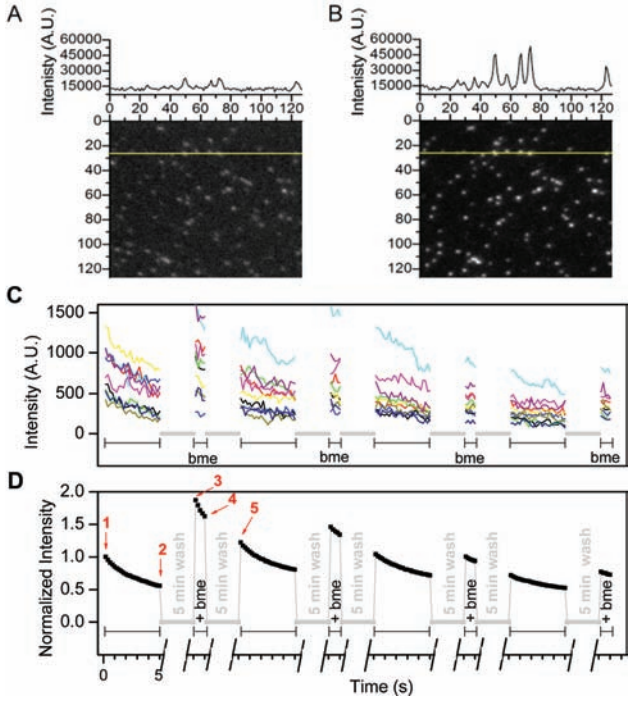

Figure 1. TIRF images of MPS-PPV supported on nanobeads (A) without and (B) with 143 mM β-mercaptoethanol (bme) in aerated buffer. The images correspond to the first frame acquired under each condition. (C) Fifteen emission intensity time trajectories acquired along cycles exchanging air-equilibrated buffer containing 0 and 143 mM β-mercaptoethanol. (D) Ensemble average trajectory for the normalized (at t = 0) fluorescence intensity of single particles along the various cycles. The average trajectory was constructed combining hundreds of traces of single nanobeads normalized to their initial intensity. The gray solid lines represent a 5 min long solution exchange period during which no photoexcitation took place.

mercaptoethanol, respectively. A line scan is shown wherefrom it is possible to appreciate a significant intensity enhancement occurring in the sample upon addition of this additive. From the series of images acquired along the time-programmed sequence, we obtained the individual particle emission intensity over time trajectories. Figure 1C shows 15 such traces randomly chosen. The trajectories were next normalized to the intensity at time 0 and combined into an ensemble average trajectory (Figure 1D).

We focused our attention on the emission intensity enhancement observed following additive incorporation (ratio of intensity at point 3 to that at point 2 in Figure 1D), the emission intensity recovery registered following incubation and rinsing of the additive (ratio of intensity at point 5 to that at point 2 in Figure 1D), and the emission intensity drop recorded following additive removal (1 − ratio of intensity at point 5 to that at point 4 in Figure 1D). These quantities were monitored and tabulated for each cycle; see Table S1 in the Supporting Information.

Upon addition of 143 mM β-mercaptoethanol, the fluorescence intensity of MPS-PPV-coated nanobeads displayed a marked enhancement in each of the four cycles recorded (for example, compare intensity points 3 and 2 in Figure 1D). To quantify the fluorescence enhancement in each cycle, we calculated for individual nanobeads the ratio of the intensity after to the intensity before introduction of β-mercaptoethanol (i.e., Figure 1D, intensity at point 3 over intensity at point 2 for

dx.doi.org/10.1021/ja208437e | J. Am. Chem.Soc. 2012, 134, 1648−1652

the first cycle). A histogram was next constructed with the enhancement recorded in hundreds of nanobeads (Figure 2A,

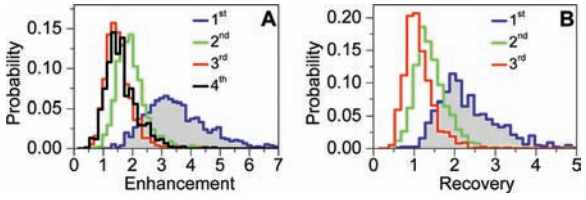

Figure 2. (A) Intensity enhancement histograms and (B) intensity recovery histograms for cycles of buffer and buffer + 143 mM β-mercaptoethanol. Histograms are shown in blue, red, green, and black on going from the first to the fourth cycle, respectively. The enhancement is calculated by dividing the intensity recorded upon addition of 143 mM β-mercaptoethanol by the intensity prior to its addition. The recovery measures the ratio of emission intensity after to emission intensity before additive incorporation.

blue). In the first cycle, the replacement of the buffer by β-mercaptoethanol resulted in a 3.5-fold intensity enhancement of MPS-PPV-coated nanobeads. The enhancement decreased from 3.5-fold to 1.9-fold in the second cycle (Figure 2A, red), and after the second cycle it leveled at 1.5-fold. The low MPS-PPV fluorescence intensity recorded upon prolonged laser illumination after four consecutive cycles prevented an accurate quantification of the ratios in subsequent cycles. We also note that β-mercaptoethanol did not stop the photodegradation of the polymer since the reduction in emission intensity over time was the same with or without this additive.

Following removal of β-mercaptoethanol, the first intensity point acquired showed a ca. 30% drop in emission intensity (compare points 4 and 5 in Figure 1D). The intensity enhancement and intensity drop experienced with the addition and removal, respectively, of β-mercaptoethanol are consistent with dynamic quenching of MPS-PPV triplet states by this additive. Triplet states are long-lived dark states; their elimination increases the duty cycle of a fluorophore, raising the overall intensity output over time.

It may be observed in Figure 1D that the drop in intensity did not restore the emission to its value immediately before addition of β-mercaptoethanol (compare points 5 and 2), indicating that a fluorescence intensity recovery took place in photoirradiated MPS-PPV coated onto nanobeads (see Figure 2B for the intensity recovery histogram for all particles analyzed). The fluorescence intensity recovery was most noticeable in the first of the four cycles and negligible in the last cycle recorded. To minimize the effect of photodegradation in measuring the emission intensity recovery, we recorded the intensity in three different pristine regions of the MPS-PPV-coated nanobead sample, first in buffer, next after β-mercaptoethanol was incubated for 5 min, and finally upon extensive washing of the nanobeads with buffer. Histograms of particle emission intensity acquired under these three conditions showed a ~2.2-fold fluorescence recovery (see the Supporting Information, Figure S1). The intensity recovery may not be explained by the triplet quenching action of β-mercaptoethanol, which was efficiently removed from the sample. It rather reflects the scavenging by β-mercaptoethanol of nonemissive traps formed along the backbone of MPS-PPV supported on SiO_2 nanobeads.

Aldehydes and dioxetanes are nonemissive traps introduced into PPV polymers upon photoirradiation under an oxygen atmosphere. Under these conditions singlet oxygen is sensitized and next undergoes a cycloaddition to the double bond connecting the phenylene moieties to form a dioxetane. The dioxetane in turn rapidly decomposes, leading to formation of aldehydes concomitant with chain scission (Scheme 1).[2b,3c] It is plausible that under our experimental conditions dioxetanes and carbonyl defects within the polymer backbone, formed during sample preparation and/or generated upon prolonged irradiation, are rapidly scavenged in the presence of β-mercaptoethanol. The facile and quantitative reduction of dioxetanes by thiols in water has been reported to take place, yielding the vicinal diols as the main product.[19] Nucleophilic addition to aldehydes, yielding thioacetals, has been further reported (see Scheme 2). The formation of vicinal diols or

Scheme 2. Plausible Reactions of β-Mercaptoethanol with Nonemissive Traps in MPS-PPV: (A) Dioxetane,[19] (B) Aldehyde

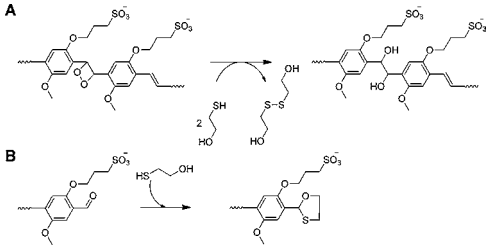

thioacetals in the presence of β-mercaptoethanol would destroy the nonemissive traps, thus restoring the emission of the MPS-PPV supported on the SiO_2 nanobeads.

We next investigated the effects of ascorbic acid and sodium azide in air-equilibrated solutions and that of β-mercaptoethanol in an oxygen-free atmosphere achieved with an enzymatic ground-state oxygen scavenger consisting of glucose oxidase, catalase, and β-D-(+)-glucose. Figure 3 provides the ensemble average trajectory for the normalized fluorescence intensity of single particles, and the intensity enhancement and intensity recovery histograms for cycles involving the addition and removal of the above additive combinations. The emission intensity enhancement, recovery, and drop are further tabulated in Table S1 in the Supporting Information. In all cases a marked emission enhancement and emission recovery were recorded in the first cycle. This may be the result of the reduction by the various additives of nonemissive traps formed along the MPS-PPV backbone during sample preparation and/or storage. Alternatively, it may arise from the scavenging, by additives, of exciton traps within the SiO_2 architecture.

For ascorbic acid in air-equilibrated solutions, we recorded an emission enhancement in all cycles upon its introduction (Figure 3A–C), but we observed no drop in emission intensity concomitant with the removal of this additive in all but the first cycle. This observation is in stark contrast to results obtained with β-mercaptoethanol in air-equilibrated solutions. Also, we note that only a minor (3% per second) reduction in intensity over time was noticeable upon excitation of the sample in the presence of ascorbic acid. Ascorbic acid is thus shown to play no role in the dynamic quenching of triplet states (no drop in intensity was observed immediately after the additive was removed) but rather a significant role in the polymer emission recovery. Presumably, the emission recovery with ascorbic acid (as well as that observed with β-mercaptoethanol) arises from the reduction of dioxetanes[19b] formed upon the reaction of the

dx.doi.org/10.1021/ja208437e | J. Am. Chem.Soc. 2012, 134, 1648–1652

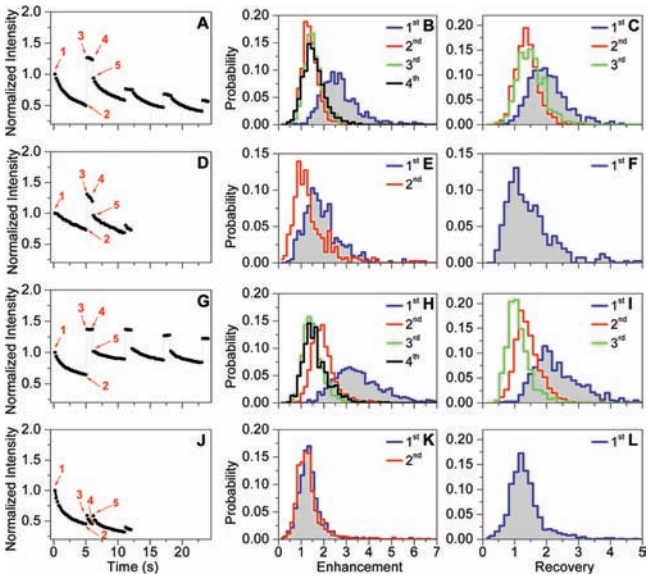

Figure 3. From left to right, ensemble average trajectory for the normalized fluorescence intensity of single particles, enhancement histograms, and recovery histograms for cycles exchanging buffer and buffer + 100 mM ascorbic acid (A–C), cycles exchanging buffer and buffer + 100 mM sodium azide (D–F), cycles exchanging an enzymatic oxygen scavenger and enzymatic oxygen scavenger + 143 mM β-mercaptoethanol (G–I), and a control sample where only buffer is flowed (J–L). The 5 min solution exchange periods in panels A, D, G, and J were truncated in the average trajectory plots to facilitate display.

polymer with singlet oxygen and which otherwise act as nonemissive exciton traps[6] (recent results show that reducing agents also lead to fluorescence recovery in single-walled carbon nanotubes by virtue of passivation of defect sites[20]). The minor intensity reduction recorded with ascorbic acid over time is consistent with the additive also acting as a singlet oxygen scavenger, preventing polymer photodamage.

For sodium azide, rapid degradation of the sample prevented conduction of more than one full observation cycle (Figure 3D–F). In the presence of this additive, the emission enhancement was significant (intensity at points 3 and 2) but the emission recovery was moderate with an intensity ratio of 1.4 measured before and after additive removal. Further sodium azide did not prevent the photodegradation of the polymer as can be observed from the reduction in intensity over time in the presence of this additive (compare intensity points 4 and 3). The rate of intensity loss recorded with and without sodium azide was the same, ca. 10% per second.

For an oxygen-free atmosphere, the reduction in emission intensity/polymer photodamage with time (ca. 3% per second) was significantly smaller than in air-equilibrated samples as can be observed when we compare panel G with panels A and D of Figure 3 in those segments where no additives were added. Addition of β-mercaptoethanol to the solution containing the enzymatic oxygen scavenger resulted in a significant intensity enhancement and negligible reduction in intensity over time (less than 1% per second). We calculated for each cycle the average intensity drop of MPS-PPV upon rinsing β-mercaptoethanol and estimate that this additive, acting as a triplet quencher, enhances the fluorescence intensity of MPS-PPV by 30%, which is comparable to values obtained for β-mercaptoethanol in air-equilibrated solutions (see above). We may also note upon comparing the intensity recovery values due to β-mercaptoethanol for an air-equilibrated vs oxygen-free atmosphere that in the latter case the recoveries are initially less pronounced but constant over the cycles (see also Figures 1D and 3G), which is consistent with reduced photodamage in an oxygen-free atmosphere.

To rule out the occurrence of a photostationary dark or trap state formed upon excitation[21] and which rapidly recovers in an additive-independent manner during the 5 min nonilluminated wash period, we performed a control experiment that involved addition of buffer rather than any of the additives above-mentioned (see Figure 3, bottom panel and Table S1 in the Supporting Information). Given the significant photobleaching observed, only two cycles were recorded. Under these conditions there is a minor enhancement and recovery which point to a minor contribution from the formation of a dark photostationary state.

Control ensemble studies with ethylene glycol further enabled us to rule out conformational changes along the MPS-PPV backbone[18b,c,22] as the source for the enhanced photostability and fluorescence intensity which is recorded with β-mercaptoethanol. Ethylene glycol, an analogue of β-mercaptoethanol, lacks the triplet quenching capability arising from the heavy atom effect of the thiol moiety.[9] The control experiments showed that β-mercaptoethanol, but not ethylene glycol, enhanced the photostability of MPS-PPV (see the Supporting Information, Figure S2).

CONCLUSIONS

In summary, applying a time-programmed sequence involving addition and removal of different additives, we have shown that both β-mercaptoethanol and ascorbic acid are able to repair photodamaged MPS-PPV when supported on SiO_2 nanobeads and that additionally β-mercaptoethanol exerts a triplet quenching effect which leads to enhanced emission intensity in the presence of this additive. Addition of an enzymatic ground-state oxygen scavenger suppresses the polymer photodamage, and under these conditions β-mercaptoethanol is shown to enhance by up to 3-fold the emission intensity of the nanobeads. Furthermore, little to no photodamage is observed under these conditions, which we find optimal for developing single-molecule fluorescence-based assays relying on the emission of these nanoparticles. Overall, the single-particle imaging approach we have developed enabled us to study the photochemical and photophysical behavior of MPS-PPV-coated SiO_2 nanobeads under a range of conditions in a number of cycles. This platform is uniquely poised to address the photophysical behavior of multiple conjugated polyelectrolyte-coated SiO_2 nanoparticles in parallel fashion.

EXPERIMENTAL SECTION

MPS-PPV-Coated Nanobead Preparation Procedure. The general procedure for the nanobead preparation was recently reported[16] and is detailed in the Supporting Information.

Time-Programmed Sequence Single-Particle Imaging Procedure. Samples were imaged using an Olympus IX71 inverted microscope adapted with the Olympus commercial turnkey TIRF module IX2-RFAEVA-2. The samples were illuminated at the critical angle using the 488 nm output of a continuous-wave (cw) Ar^+ laser from SpectraPhysics. The laser beam was introduced via a single-mode fiber optic and directed by a dichroic beam splitter (z488rdc, Chroma, Rockingham, VT) to the sample via a high numerical aperture (NA = 1.45) oil immersion objective (Olympus PLAN APO 60X). Fluorescence emission was collected through the same objective and

dx.doi.org/10.1021/ja208437e | J. Am. Chem.Soc. 2012, 134, 1648–1652

then transmitted through an emission filter, HQ530 LP, into a Cascade 512B EMCCD camera (Roper Scientific, Inc.) operated with Image Pro software. Individual beads were identified using a customized Matlab program to obtain the intensity time trace and correct for the drifting of the sample.

Coverslips were cleaned in piranha solution (25% (v/v) H_2O_2, 30% and 75% (v/v) concentrated H_2SO_4) and rinsed first with distilled deionized water and next with acetone (99.5% high-performance liquid chromatography (HPLC) grade, ACP Chemicals, Montreal, Quebec, Canada). The clean coverslips were then incubated in a 2% (v/v) solution of Vectabond (Vector Laboratories, Burlingame, CA) in acetone for 5 min. The reaction was quenched by replacing the acetone with water and rinsing twice. Coverslips were rinsed with HyPure molecular biology grade water (HyClone, Logan, UT) and dried under an argon stream. Flow chambers prepared with a predrilled polycarbonate film (Grace Bio-Laboratories, Bend, OR) were next assembled on top of the coverslips, yielding 10 μL chambers. Inlet and outlet silicone ports were glued on top of the chamber with double-sided tape.

A total of 20−40 μL of a 10 pM bead solution was first injected into the chambers; subsequently 20 μL of buffer solution consisting of 150 mM NaCl and 10 mM Tris−HCl, pH 8.0, was injected to remove any beads not bound to the surface. Images were recorded at a 200 ms integration time and 3200 on-chip gain, and the power of the 488 nm Ar^+ laser utilized was 850 μW when measured at the front end of the objective with the laser in the vertical position. Samples were imaged for 5 s, during which the buffer solution was flowing at a 5 μL/min rate. Subsequently, a wash period was performed in which the additives (143 mM β-mercaptoethanol, 100 mM ascorbic acid, or 100 mM sodium azide) in buffer solutions were flowed in the dark at 20 μL/min for 5 min. The same region was then imaged for 1 s, during which the additive-enriched solution was flowing at a 5 μL/min rate. Finally, a wash period was performed in which the buffer solution was flowed in the dark at 20 μL/min for 5 min. This procedure was then repeated so that up to four cycles of imaging in buffer only followed by imaging in additive-enriched buffer solution were performed. All experiments were conducted at room temperature (22 °C). The MPS-PPV-coated nanobeads were imaged in aerated solutions unless otherwise specified. An enzymatic ground-state oxygen scavenger consisting of 0.1 mg/mL glucose oxidase, 0.02 mg/mL catalase, and 3% (w/w) β-D-(+)-glucose was used when specified.

■ ASSOCIATED CONTENT

Ⓢ Supporting Information

Nanobead preparation, intensity recovery studies, ensemble photostability studies, and time-programmed sequence movie. This material is available free of charge via the Internet at http://pubs.acs.org.

■ AUTHOR INFORMATION

Corresponding Author

gonzalo.cosa@mcgill.ca

■ ACKNOWLEDGMENTS

G.C. is grateful to the Natural Sciences and Engineering Research Council and Canadian Foundation for Innovation New Opportunities Fund for financial assistance. A.T.N. is thankful to the McGill Chemical Biology Fellowship Program (CIHR) and FQRNT for postgraduate scholarships. H.-W.L. is thankful to the McGill CIHR Training in Drug Development Program for a Postdoctoral Fellowship.

■ REFERENCES

(1) (a) Hu, D.; Yu, J.; Barbara, P. F. *J. Am. Chem. Soc.* **1999**, *121*, 6936. (b) Yu, J.; Hu, D. H.; Barbara, P. F. *Science* **2000**, *289*, 1327. (c) VandenBout, D. A.; Yip, W. T.; Hu, D. H.; Fu, D. K.; Swager, T. M.; Barbara, P. F. *Science* **1997**, *277*, 1074.

(2) (a) Burrows, H. D.; Melo, J. S. d.; Serpa, C.; Arnaut, L. G.; Monkman, A. P.; Hamblett, I.; Navaratnam, S. *J. Chem. Phys.* **2001**, *115*, 9601. (b) Scurlock, R. D.; Wang, B.; Ogilby, P. R.; Sheats, J. R.; Clough, R. L. *J. Am. Chem. Soc.* **1995**, *117*, 10194.

(3) (a) Dam, N.; Scurlock, R. D.; Wang, B.; Ma, L.; Sundahl, M.; Ogilby, P. R. *Chem. Mater.* **1999**, *11*, 1302. (b) Candeias, L. P.; Wildeman, J.; Hadziioannou, G.; Warman, J. M. *J. Phys. Chem. B* **2000**, *104*, 8366. (c) Burrows, H. D.; Narwark, O.; Peetz, R.; Thorn-Csanyi, E.; Monkman, A. P.; Hamblett, I.; Navaratnam, S. *Photochem. Photobiol. Sci.* **2010**, *9*, 942.

(4) Cornil, J.; dos Santos, D. A.; Crispin, X.; Silbey, R.; Brédas, J. L. *J. Am. Chem. Soc.* **1998**, *120*, 1289.

(5) Stringle, D. L. B.; Campbell, R. N.; Workentin, M. S. *Chem. Commun.* **2003**, 1246.

(6) Park, S. J.; Gesquiere, A. J.; Barbara, P. F. Fabrication, Physics, and Chemistry toward Organic Nanophotonics. In *Nanophotonics: Integrating Photochemistry, Optics and Nano/Bio Materials Studies*; Masuhara, H., Kawata, S., Eds.; Proceedings of the 1 International Nanophotonics Symposium: Handai, Osaka, Japan, 2004; Vol. *1*.

(7) Chambon, S.; Rivaton, A.; Gardette, J.-L.; Firon, M. *J. Polym. Sci., Part A: Polym. Chem.* **2009**, *47*, 6044.

(8) (a) Selvin, P. R.; Ha, T. *Single-Molecule Techniques: A Laboratory Manual*, 1st ed.; Cold Spring Harbor Laboratory Press: Cold Spring Harbor, NY, 2008; (b) Rasnik, I.; McKinney, S. A.; Ha, T. *Nat. Methods* **2006**, *3*, 891.

(9) (a) Bohne, C.; Alnajjar, M. S.; Griller, D.; Scaiano, J. C. *J. Am. Chem. Soc.* **1991**, *113*, 1444. (b) Becker, R. S.; Jordan, A. D.; Kolc, J. *J. Chem. Phys.* **1973**, *59*, 4024.

(10) Vogelsang, J.; Kasper, R.; Steinhauer, C.; Person, B.; Heilemann, M.; Sauer, M.; Tinnefeld, P. *Angew. Chem., Int. Ed.* **2008**, *47*, 5465.

(11) (a) Cordes, T.; Vogelsang, J.; Tinnefeld, P. *J. Am. Chem. Soc.* **2009**, *131*, 5018. (b) Campos, L. A.; Liu, J.; Wang, X.; Ramanathan, R.; English, D. S.; Munoz, V. *Nat. Methods* **2011**, *8*, 143.

(12) Landry, M. P.; McCall, P. M.; Qi, Z.; Chemla, Y. R. *Biophys. J.* **2009**, *97*, 2128.

(13) (a) Harada, Y.; Sakurada, K.; Aoki, T.; Thomas, D. D.; Yanagida, T. *J. Mol. Biol.* **1990**, *216*, 49. (b) Ha, T. *Methods* **2001**, *25*, 78.

(14) Andrew, T. L.; Swager, T. M. *Macromolecules* **2008**, *41*, 8306.

(15) Decher, G. *Science* **1997**, *277*, 1232.

(16) Ngo, A. T.; Lau, K. L.; Quesnel, J. S.; Aboukhalil, R.; Cosa, G. *Can. J. Chem.* **2011**, *89*, 385.

(17) (a) Chemburu, S.; Ji, E.; Casana, Y.; Wu, Y.; Buranda, T.; Schanze, K. S.; Lopez, G. P.; Whitten, D. G. *J. Phys. Chem. B* **2008**, *112*, 14492. (b) Wosnick, J. H.; Liao, J. H.; Swager, T. M. *Macromolecules* **2005**, *38*, 9287. (c) Zeineldin, R.; Piyasena, M. E.; Bergstedt, T. S.; Sklar, L. A.; Whitten, D.; Lopez, G. P. *Cytometry, Part A* **2006**, *69A*, 335. (d) Zeineldin, R.; Piyasena, M. E.; Sklar, L. A.; Whitten, D.; Lopez, G. P. *Langmuir* **2008**, *24*, 4125.

(18) (a) Huser, T.; Yan, M.; Rothberg, L. J. *Proc. Natl. Acad. Sci. U.S.A.* **2000**, *97*, 11187. (b) Karam, P.; Ngo, A. T.; Rouiller, I.; Cosa, G. *Proc. Natl. Acad. Sci. U.S.A.* **2010**, *107*, 17480. (c) Ngo, A. T.; Karam, P.; Cosa, G. *Pure Appl. Chem.* **2011**, *83*, 43.

(19) (a) Adam, W.; Epe, B.; Schiffmann, D.; Vargas, F.; Wild, D. *Angew. Chem., Int. Ed.* **1988**, *27*, 429. (b) Adam, W.; Vargas, F.; Epe, B.; Schiffmann, D.; Wild, D. *Free Radical Res.* **1989**, *5*, 253.

(20) Lee, A. J.; Wang, X.; Carlson, L. J.; Smyder, J. A.; Loesch, B.; Tu, X.; Zheng, M.; Krauss, T. D. *Nano Lett.* **2011**, *11*, 1636.

(21) Gensch, T.; Böhmer, M.; Aramendía, P. F. *J. Phys. Chem. A* **2005**, *109*, 6652.

(22) (a) Ngo, A. T.; Cosa, G. *Langmuir* **2010**, *26*, 6476. (b) Ngo, A. T.; Karam, P.; Fuller, E.; Burger, M.; Cosa, G. *J. Am. Chem. Soc.* **2008**, *130*, 457.